Child Activity Recognition Based on Cooperative Fusion Model of a Triaxial Accelerometer and a Barometric Pressure Sensor

Yunyoung Nam and Jung Wook Park

***Abstract*—This paper presents a child activity recognition approach using a single 3-axis accelerometer and a barometric pressure sensor worn on a waist of the body to prevent child accidents such as unintentional injuries at home. Labeled accelerometer data are collected from children of both sexes up to the age of 16 to 29 months. To recognize daily activities, mean, standard deviation, and slope of time-domain features are calculated over sliding windows. In addition, the FFT analysis is adopted to extract frequency-domain features of the aggregated data, and then energy and correlation of acceleration data are calculated. Child activities are classified into 11 daily activities which are wiggling, rolling, standing still, standing up, sitting down, walking, toddling, crawling, climbing up, climbing down, and stopping. The overall accuracy of activity recognition was 98.43% using only a single-wearable triaxial accelerometer sensor and a barometric pressure sensor with a support vector machine.**

***Index Terms*—Accelerometer, activity classification, activity recognition, baby care, child care, wearable device.**

I. Introduction

As BABIES usually start walking between 9 and 16 months, they are at risk of falling from furniture or stairs. As toddlers learn to climb, they are at risk of falling from windows and beds. Falls are a frequent cause of injury in children. Accident and emergency departments and outpatient surveillance systems show that falls are one of the most common mechanisms of injuries that require medical care, and the most common nonfatal injury that at times needs hospitalisation. In children younger than four years of age, most fall-related injuries occur at home. Thus, a new safety management method for children is required to prevent child home accidents. Since the major causes of fall-related injuries change as a child grows and develops, fall prevention needs to be addressed. One of the most challenging issues in this context is to classify daily activities of children into safe and dangerous activities.

Although numerous approaches [1]–[3] have proposed various activity recognition methods, human activity recognition is one of the challenging issues in terms of accurate recognition. In general, a pervasive safety management system aims to reduce risk factors of injuries to prevent accidents by using smart sensors. Multisensor fusion has been applied to daily life monitoring for elderly people and children at home [4], [5]. This approach trained using manually annotated data and applied for activity recognition. Zhu *et al.* [6] also suggested human activity recognition by fusing two wearable inertial sensors attached to one foot and the waist of a human subject, respectively. The use of multiple sensors has been shown to improve the robustness of the classification systems and enhance the reliability of the high-level decision making. On the other hand, a waist-worn sensor could fail to detect activities involving head motion, body tilt, and hand motion. In addition to that and for the purpose of minimizing the number of sensors worn, it is important to know the capability of a certain position to classify a set of activities.

Recently, Atallah *et al.* [7] investigated the effects of sensor position and feature selection on activity classification tasks using accelerometers. Accelerometers are not only the most broadly used sensors to recognize ambulation activities such as walking and running, but also inexpensive, require relatively low power, and are embedded in most of cellular phones. Their study concluded that optimal sensor positions depend on the activities being performed by the subject. Other important factors to consider, especially if the system is designed for long and continuous use, are how comfortable it is to wear and how easy it is to put on. Frequently, accuracy must be compromised for ease of use and comfort, due to a reduction in number of sensors. The optimal system configuration is, therefore, difficult to evaluate. It depends not only on the accuracy of the system but also on other practical aspects. In our study, for children under three years of age, the waist-worn sensor is put in a diaper to minimize uncomfortableness during physical activity and to measure body motions such as climbing up and climbing down than head, hand, and leg motions.

We have developed a wearable sensor device and a monitoring application to collect information and to recognize baby activities. We classified baby activities into 11 daily activities which are wiggling, rolling, standing still, standing up, sitting down, walking, toddling, crawling, climbing up, climbing down, and stopping. Multiple sensors embedded in a wearable device

Manuscript received March 24, 2012; revised August 27, 2012; October 26, 2012; accepted December 10, 2012. Date of publication January 9, 2013; date of current version March 8, 2013. This work was supported by the International Collaborative R&D Program of the Ministry of Knowledge Economy, the Korean Government, as a result of development of security threat control system with multisensor integration and image analysis under Project 2010-TD-300802-002.

Y. Nam is with the Department of Electrical and Computer Engineering, Stony Brook University, Stony Brook, NY 11794 USA (e-mail: young022@gmail.com).

J. W. Park is with the CTO Division, LG Electronics, Seoul 150-721, Korea (e-mail: ubihuman@gmail.com).

Color versions of one or more of the figures in this paper are available online at http://ieeexplore.ieee.org.

Digital Object Identifier 10.1109/JBHI.2012.2235075

TABLE I
SENSOR TYPES OF THE WEARABLE SENSOR DEVICE

Type	Sensor	Value	Feature
Space	RFID	ID	Location (e.g. living room, dining room)
Object	RFID	ID	Object Name (e.g. electric socket)
Activity	3-axis accelerometer	[-2g, +2g]	Activity (e.g. toddling, standing)
Height	Absolute pressure sensor	[30kPa, 129kPa]	Height from the ground
Temperature	Temperature sensor	[-40°C, 125°C]	Ambient temperature

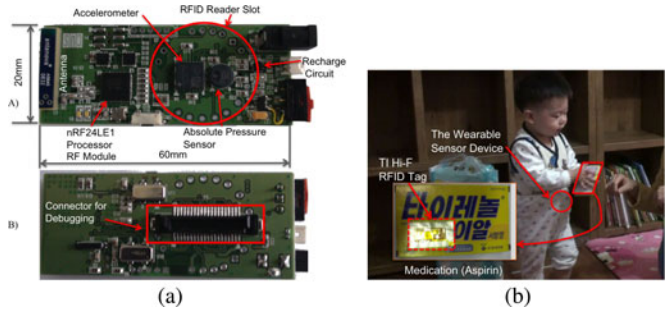

Fig. 1. Prototype of the wearable sensor device and the RFID tag. (a) Wearable sensor device. (b) Device and the RFID tag.

are more accurate for collecting different types of sensing information [8], but would be very inconvenient for users. For this reason, we present only one single unit of sensor nodes, which collects multiple types of information.

The nature of information interaction involved in sensor fusion can be classified as competitive, complementary, and cooperative fusion [9]–[11]. In competitive fusion, each sensor provides equivalent information about the process being monitored. In complementary fusion, sensors do not depend on each other directly, as each sensor captures different aspects of the physical process. The measured information is merged to form a more complete picture of the phenomenon. Cooperative fusion of the two sensors enables recognition of the activity that could not be detected by each single sensor. Due to the compounding effect, the accuracy and reliability of cooperative fusion is sensitive to inaccuracies in all simple sensor components used. In this paper, we select the cooperative fusion model to combine information from sensors to capture data with improved reliability, precision, fault tolerance, and reasoning power to a degree that is beyond the capacity of each sensor.

The main contributions of this paper over the earlier previous work are 1) to extend the method to work with arbitrary every day activities not just walking by improving the feature selection and recognition procedure; 2) to perform evaluation on a large (50 h) dataset recorded from real life activities; 3) to have studied ten divers subjects: 16, 17, 20, 25, 27 months-old baby boys and 21, 23, 24, 26, 29 months-old girls; and 4) to employ a barometric pressure sensor for improving upon the previous algorithms. The proposed method classified daily physical activity of children by a diaper worn device consisting of a single-triaxial accelerometer and a barometric air pressure sensor. We demonstrate our improvements in comparison to the accuracy results of only a single-wearable device and multiple feature sets to find an optimized classification method.

II. METHODS

A. Sensor Device

In order to recognize daily activities, we adopt multiple sensors, as shown in Table I, as follows: 1) a 3-axis accelerometer measures the movement; 2) an absolute pressure sensor measures absolute pressure enabling a measurement of a distance between the ground and the wearable sensor device; 3) a radio-frequency identification (RFID) (SkyeModule M1-mini) is selected to read/write tags and smart labels, which has compatibility with most industry standard 13.56 MHz.

We used the SCA3000 that is a 3-axis accelerometer for applications requiring high performance with low power consumption. It consists of three signal-processing channels where it is low-pass filtered and communicates with the processing layer based on SPI bus that is a full duplex synchronous 4-wire serial interface. We also used the SCP1000 as a pressure sensor that measures absolute pressure to measure distance between the ground and the sensor. The pressure and temperature output data are calibrated and compensated internally. The sensor communicates with the processing layer through an SPI bus. The SkyeModule M1-mini has a read/write distance that is typically greater than or equal to two inches for an ISO15693 RFID inlay. The sensor allows us to recognize objects and space that may cause dangerous situations. Finally, we developed the prototype wearable sensor device (size of 65mm $\times$ 25 mm) including the dual-core processor and sensors as shown in Fig. 1.

B. System Architecture

The proposed system consists of four main components: 1) the wearable sensor node to measure movement and height from the ground by using a 3-axis accelerometer and a pressure sensor; 2) the wireless receiver to receive the measured data over Nordic wireless protocol and transmit it to PC over USB connection; 3) the activity monitor and analyzer working on the PC to aggregate the measured raw data and to analyze behavioral characteristics using features and classifiers; and 4) the speaker to broadcast emergency alerts to their parents or a guardian.

The proposed activity recognition method using a 3-axis accelerometer and a pressure sensor comprises the following three steps: 1) collecting and preprocessing the sensor data from an accelerometer; 2) extracting features; and 3) training and classification. In order to process, we have to remove the noise with a moving-average filter because errors made in the early steps may increase the classification error and the uncertainty on each further step. After preprocessing the sensors signals, it is necessary to choose the adequate features which we take as time-domain and frequency-domain features.

C. Feature Extraction

Let X, Y, and Z denote the infinite data stream of measured acceleration values of the three space dimensions

$$X = (x_1, x_2, \ldots), \quad Y = (y_1, y_2, \ldots), \quad Z = (z_1, z_2, \ldots). \tag{1}$$

The corresponding data stream M of the magnitude is defined as

$$M = (m_1, m_2, \ldots)$$
$$\text{where } m_i = \sqrt{x_i^2 + y_i^2 + z_i^2}. \tag{2}$$

The magnitude of the force vector is calculated by combining the measurements from all three axes using (2) to derive acceleration independent of orientation. A sliding window of the size n is pushed through the values of the incoming data stream with a specified offset. Suppose that $X' = (x'_1, \ldots, x'_n)$ refers to the acceleration signals in the direction of the x-axis observed in the sliding window at a certain time. Y', Z', and M' are defined analogously.

To extract features of the experimental data, we set the window size to 256 and sample overlapping between consecutive windows to 128 at 95 Hz sampling frequency. The window size represents the time duration of the accelerometer data that is needed to distinguish an activity. When the size is fixed, with small window size, the decision is made with the information within short time duration and the features may be insufficient to describe an activity. On the contrary, with large size, the decision is made with large amount of features over long time duration and with limited training data, it may cause overfitting problems. So, there should be a suitable window length that could achieve the best tradeoff. To choose the best window size, we evaluated the window size from 32, 64, 128, 256, and 512 samples. We found out that the precision achieves the peak 95% when the window size is 256 samples. When the window size is smaller or larger, the precision decreases. Thus, the windows used for feature extraction were selected to be 256 samples (2.7 s) in our study.

1) Noise Reduction: The obtained time series signal consists of lots of noise caused by unnecessary movement. The effect of the jittering noise can be reduced by scaling down (x', y', z') readings, followed by a smoothing technique using a moving-average filter *mv-filter* of span L, as follows:

$$(x'', y'', z'') = \text{mv-filter}((x', y', z'), L). \tag{3}$$

The moving-average filter smooths data by replacing each data with the average of the neighboring data defined within L. The moving-average filter operates by averaging a number of points from the input signal to produce each point in the output signal. It can be seen that the proposed smoothing technique greatly removes the jittering noise and smooths out data by more significant standard deviation reduction than mean reduction.

The smoothing action of the moving average filter decreases the amplitude of the random noise, but also reduces the sharpness of the edges. The moving average produces the lowest noise for a given edge sharpness. The amount of noise reduction is equal to the square-root of the number of points in the average. The smoothing parameters can be interactively tuned by experience with a tradeoff between smoothing and sharpness preserving. In order to determine the optimal size of the moving filter window, three series of the input signals were smoothed by the moving average filter using span parameter 3, 5, and 9, respectively. From empirical observation, the five-point averaging was found to be optimal.

TABLE II
STATISTICS OF AN ACCELEROMETER

Activity	$\sigma_{x''}$	$\sigma_{y''}$	$\sigma_{z''}$	σV	σH
Walking	18.63	10.55	12.17	20.42	6.43
Crawling	8.34	5.81	5.33	11.01	4.47
Climbing up	50.63	37.66	19.42	45.03	7.46
Climbing down	56.93	32.99	18.15	45.24	7.76

2) Time-Domain Feature: The gravity component is estimated from each segment of (x', y', z') readings. Our estimation interval is set to the same as sample duration, which is to estimate the vertical acceleration vector $\bar{v}_{\text{norm}}$ corresponding to gravity as $\bar{v} = (mx', my', mz')$, where mx', my', and mz' are averages of all the measurements on those respective axes for the sampling interval. Let $\bar{a}_i = (x'_i, y'_i, z'_i), i = 1, 2, \ldots, N$, be the vector at a given point in the sampling interval, where N is the length of sample points in the sample duration. The projection of $\bar{a}_i$ onto the vertical axis $\bar{v}_{\text{norm}}$ can be computed as the vertical component inside $\bar{a}_i$. Let p_i^{in} be the inner product and $\bar{p}_i$ be the projection vector, as follows:

$$p_i^{\text{in}} = < \bar{a}_i, \bar{v}_{\text{norm}} >, \bar{p}_i = p_i^{\text{in}} \cdot \bar{v}_{\text{norm}}. \tag{4}$$

Then the horizontal component $\bar{h}_i$ of the acceleration vector $\bar{a}_i$ can be computed as vector subtraction, as follows:

$$\bar{h}_i = \bar{a}_i - \bar{p}_i. \tag{5}$$

However, it is impossible to know the direction of $\bar{h}_i$ relative to the horizontal axis in global 3-axis coordinate system. We only know $\bar{h}_i$ lies in the horizontal plane that is orthogonal to estimated gravity vector $\bar{v}$. So, we simply take the magnitude of $\bar{h}_i$, denoted by $\|\bar{h}_i\|$, as a measure of horizontal movement. The results of the aforementioned algorithm generate two waveforms of $\{p_i^{\text{in}}, i = 1, 2, \ldots, N\}$ and $\{\|\bar{h}_i\|, i = 1, 2, \ldots, N\}$, which are amplitude of the vertical components and magnitude of the horizontal components, respectively. Each waveform is almost independent of orientation taking instant accelerometer samples. We mainly considered features including mean and standard deviation as Bao and Intille [8] and Ravi *et al.* [12] selected. Features were extracted from each of the three axes of the accelerometer as well as the vertical and the horizontal components, giving a total of nineteen attributes. Standard deviation was used to capture the range of possible acceleration for different activities such as walking and crawling.

Table II shows statistics of an accelerometer in walking, crawling, climbing up, and climbing down. With respect to the smoothed accelerometer data and vertical components, standard deviation of walking is greater than that of crawling. The feature characteristics of standard deviation of climbing up are very similar to that of climbing down. In other words, it is difficult to discriminate between climbing up and climbing down based

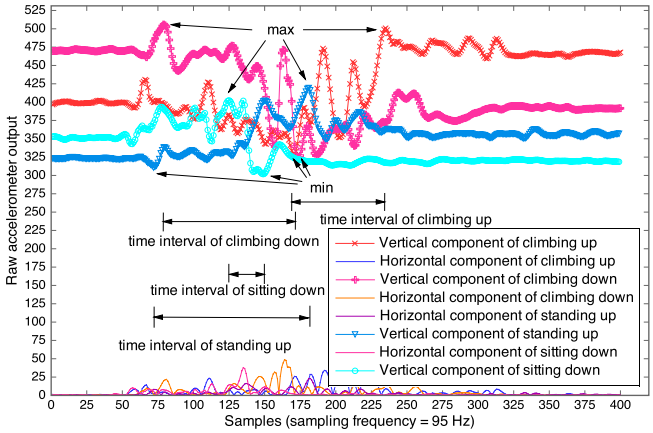

Fig. 2. Vertical and horizontal components for standing up, sitting down, climbing up, climbing down.

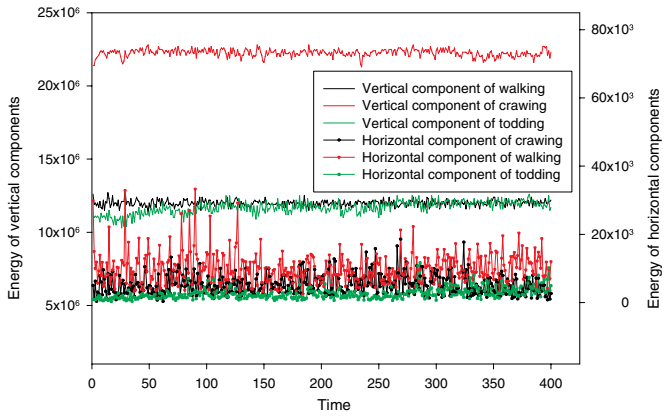

Fig. 3. Energy of vertical and horizontal components for crawling, walking, and toddling.

on standard deviation features. In this paper, the slope mapping method is used to detect whether there is apparent fluctuation in the data series. We considered a simplified trunk tilt data series $i = 1$ to n. The slope filter is used to calculate the gradient over a specified window size. The apparent changes of slopes are investigated in vertical acceleration component. The slope s_i between two neighboring data window i and $i + 1$ is calculated and a segment slope series S with $n - 1$ data window is obtained from the original n-point data series.

Fig. 2 shows examples of the vertical and horizontal acceleration components of climbing up, climbing down, standing up, and sitting down. For the climbing down case in this figure, it is observed that the maximum acceleration peak occurs prior to its minimum peak and vice versa for climbing up. This pattern exists in all samples collected in the test. Therefore, the rule is to compare the order of occurrences of those two peaks. If the maximum peak occurs prior to the minimum peak, this event could be a climbing down activity. On the contrary, if the occurrence of the maximum peak falls behind the minimum peak, the event could be a climbing up activity. Furthermore, the time interval (or peak distance) between the maximum peak and the minimum peak is considered. The time interval rule is applied for classification between standing up and sitting down activities. The sitting down activity produces shorter peak distance while the standing up activity produces longer peak distance. For example, the patterns of standing up and sitting down have the peak distances in 109 and 24, respectively.

3) Frequency-Domain Feature: We computed the frequency-domain feature of 3-axis acceleration data as well as the vertical and horizontal components. The periodicity in the data is reflected in the frequency domain. We mainly referred to successful feature extraction [8], [12], [13] based on efficient fast Fourier transform (FFT).

To capture data periodicity, the energy feature was calculated. Energy E is the sum of the squared discrete FFT component magnitudes of the signal. The sum is divided by the window length w for normalization. If $x_1, x_2, \ldots$ are the FFT components of the window, then E is calculated by

$$E = \frac{\sum_{i=1}^{w} \left| x_i^2 \right|}{|w|}. \tag{6}$$

Fig. 3 shows examples of energy of vertical and horizontal components for crawling, walking, and toddling. From this figure, it can be seen that both vertical E values of walking and toddling are around 1.2×10^7, respectively, while vertical E values of crawling is around 2.2×10^7. In the case of detecting walking and toddling, we found out that the vertical energy difference between those two states is small. However, the horizontal energy of toddling is different from that of walking. In the case of toddling, a toddler walks sideways and backward, runs well, falls, and stops easily. Thus, high peaks for the horizontal component space out at highly periodic cycles.

Correlation is especially useful for differentiating among activities that involve translation in just one dimension. For example, we can differentiate walking and running from stair climbing using correlation. Walking and running usually involve translation in one dimension whereas climbing involves translation in more than one dimension. Correlation ρ is calculated between each pair of axes as the ratio of the covariance and the product of the standard deviations by

$$\rho_{x,y} = \mathrm{corr}(x, y) = \frac{\mathrm{cov}(x, y)}{\sigma_x \sigma_y}. \tag{7}$$

We analyzed correlation coefficient between vertical and horizontal components for activities. In the case of rolling, mean and standard deviations of correlation coefficient are 0.41 and 0.13. The correlation coefficient of rolling is higher than that of other activities. In other words, the positive values of correlation coefficient indicate a stronger degree of linear relationship between vertical and horizontal variables such that as values for vertical component increases, values for horizontal component also increase.

4) Elevation Feature: The pressure sensor is used for the determination of elevation. The air pressure sensor measures the atmospheric air pressure with a resolution of 1.5 Pa, which corresponds to about 10 cm at sea level. The data obtained from the pressure sensor needs to be normalized when both indoor and outdoor activity are analyzed. However, we limited the experiment to indoor activities. The elevation data obtained from the pressure sensor are useful to detect climbing up and climbing down events. We configured pressure data of the ground as a reference value, and then the height was calculated by using

the difference between the reference and measured value. Possible pressure values ranged from 1 to 7 for climbing up and climbing down, whereas standing up and sitting down activities lies within the range of 1–5. Using this range as our region of interest, we focus on classification of climbing up and down.

D. Activity Recognition

After the feature extraction is completed, a classification procedure separates the child's activities from all other primitive features. The activity recognition algorithm should be able to recognize the accelerometer signal pattern corresponding to every activity.

1) Classification Method Using Accelerometer Data: We formulate activity recognition as a classification problem where classes correspond to activities and a test data instance is a set of acceleration values collected over a time interval and post-processed into a single instance of mean, standard deviation, energy, and correlation. In previous work to recognize activities, decision table (DT) [14], decision tree (J48) [15], support vector machine (SVM) [16], [17], and nearest neighbors [18], and Naive Bayes (NB) [19], classifiers were tested for activity recognition using the feature vector. Decision-based approaches [20], have been used in past work to recognize activities. NB is a computationally efficient algorithm that has been used for pattern classification in a variety of applications.

In this paper, we evaluated the performance of NB, Bayes Net (BN), SVM, k-nearest neighbor (k-NN), DT, J48, multilayer perceptron (MLP), and logistic regression classifiers, available in the Weka toolkit [21]. The DT learning method is one of the most widely used and practical techniques for inductive inference. The constructed tree first performs a binary split on the most salient feature (e.g., the X-axis acceleration energy from the sensor), dividing into two branches, then recursively constructs trees for each branch. The predictive values (e.g., walking, crawling, etc.) are assigned to the resulting leaves. To avoid overfitting to the data, which occurs after many tree subdivisions, since each leaf then represents only a small number of samples, the tree is pruned. The DT classifier detects errors in classification of the training samples, as well as to errors in the attribute values of the samples, which provides a good balance between accuracy and computational complexity.

2) Classification Method Using Elevation Data: The pressure sensor signal is low-pass filtered using Butterworth filter and upsampled using linear interpolation to the sampling rate of 95 Hz. The resulting signal is used to calculate the differential pressure parameter ($\Delta P[k]$). The kth sample of ΔP signal is obtained considering the average pressure during T_w (we set to 2 s) before and T_w after each sample (overlapping the windows)

$$\Delta P[k] = \frac{T_s}{T_w}\left(\sum_{i=k}^{k+\frac{T_w}{T_s}} p[i] - \sum_{i=k-\frac{T_w}{T_s}}^{k} p[i]\right) \tag{8}$$

where $p[i]$ is the ith sample of the barometric signal and T_s is the sampling period. The ΔP signal is then normalized by dividing by the height of the subject.

TABLE III
FEATURE SUBSETS AND RECOGNITION ACCURACY

Feature Set	NB	BN	SVM	J48	Logistic
M	12.4%	50.1%	7.1%	48.4%	4.6%
$mean$	24.2%	62.3%	28.7%	63.5%	29.5%
std	41%	49.9%	26.6%	54.8%	38.6%
$mean$ and std	40.3%	68.6%	49.6%	77.9%	55.6%
$mean$, std, s, E, ρ	70.6%	83.8%	82.5%	87.9%	85.1%
All	73%	84.8%	86.2%	88.3%	86.9%

If the thresholding of ΔP indicates that the device altitude has significantly changed, the event is classified as standing up, sitting down, climbing up, and climbing down. If the system recognizes that no pressure change has occurred during Tth interval, then the classification is upgraded to nonmoving status. If the system recognizes that the device altitude is significantly changed, even without detecting an activity-based acceleration data, but the ΔP exceeds a high threshold ΔPth, the event is classified as standing up, sitting down, climbing up, and climbing down.

III. RESULTS

A. Experimental Setup

Ten families were volunteered to conduct the experiment in 32.98 m^2 living room and 16.44 m^2 kitchen. In a controlled laboratory setting, all data were collected from ten babies who are 16, 17, 20, 25, 27 months-old baby boys and 21, 23, 24, 26, and 29 months-old baby girls. We recorded the experiments as videos that are synchronized with the monitoring application, and then annotated the raw data by comparing with the video. A supporter who observed the experiments annotates raw data by clicking buttons or typing name of the activities through the monitoring application. All experiments were performed in a real home environment consisting of one wearable sensor device for the child and the monitoring application operated on a laptop computer.

Baby boys wiggled more than baby girls. They squirmed more and get restless on the floor, and crawl over longer distances. While the average boy did not move around much more than the typical girl, the most active children were almost always boys, and the least active children were girls. Based on 2003–2006 NHANES data [22], the average height between two and three years old children is set to 94.725 cm. Also, the chest height is set to 94.725·3/4 cm. From empirical observation, we assume that 70 cm is set to the height from the ground where children can climb up themselves.

B. Experimental Results

There were total 1538 samples collected from one baby as training data. The other samples collected from ten babies were used as a test dataset. We evaluated and compared several classifiers as mentioned in Section II-D1. Ten-fold cross validation was also used for testing. Different feature subsets are listed in Table III. From the accuracy results, mean and standard deviation features contained more motion information than M features because vertical and horizontal features can detect

TABLE IV
RECOGNITION RESULT COMPARISON, (a) STANDING STILL, (b) STANDING UP, (c) SITTING DOWN, (d) WALKING, (e) TODDLING, (f) CRAWLING, (g) CLIMBING UP, (h) CLIMBING DOWN, (i) STOPPING, (j) WIGGLING, AND (k) ROLLING

Classifier	a	b	c	d	e	f	g	h	i	j	k	Average
NB	64.9%	28%	74.7%	90.9%	71%	84.3%	62%	83.3%	79.7%	78.3%	84.2%	73%
BN	90.4%	81.5%	90.1%	90.3%	91.5%	98.9%	57.8%	58%	96.2%	90.3%	97.7%	84.8%
SVM	99.2%	95.4%	97.6%	97.2%	96.7%	96.8%	39.8%	48.7%	97.8%	95.9%	99.9%	86.2%
KNN	90.4%	82.2%	89.1%	83.5%	77%	89.1%	67.8%	69.4%	91.8%	93.4%	94.6%	84.1%
J48	97.5%	85.2%	88.5%	90.6%	91.4%	92.6%	71.7%	71.8%	95.5%	93.8%	98.7%	88.3%
DT	54.6%	74.3%	82.9%	81.2%	80.7%	86.5%	39.5%	52.8%	89.4%	84.1%	97.2%	74%
MLP	75.6%	99.5%	93.1%	93.4%	97.2%	99.9%	63.6%	52.5%	98.9%	77.8%	93.7%	84.8%
Logistic	94.4%	87.5%	86.8%	87.1%	85.5%	91.2%	74.7%	72.1%	91.8%	90.3%	98.7%	86.9%
ΔP	-	99.9%	99.8%	-	-	-	99.9%	99.6%	-	-	-	

movement better than M features. Most classifiers using all features can better distinguish activities than that of using only time-domain features. Although Logistic achieved high-recognition accuracy, these classifiers took 158.35 s to build a model. We analyzed precision and computational time of an SVM depending on complexity parameters. The SVM achieved high-recognition accuracy when complexity parameter was 10 000. However, the classifier took 170.72 s to build a model. BN and DT were found to achieve high- recognition accuracy with acceptable computational complexity. They are computationally efficient, and their performance is suitable for real-time recognition.

Table IV shows that we achieved high levels of accuracy in most cases. For most common activities, we generally achieved accuracies above 90% except NB. The classification between walking and toddling activities is more difficult than the classification between other activities. This can be partially explained by the similarity of these two activities and the basic characteristics of child activities such as unintended moving. Two activities may be considered the same activity in point of view, and can be considered only for moving detection. However, in this paper, two activities are classified by the horizontal energy, consequently, we achieved accuracies above 90% based on the BN, SVM, J48, and MLP classifiers.

Crawling appears easier to identify than walking, which seems to make sense, since crawling involves more horizontal changes in acceleration. It appears much more difficult to identify climbing up and climbing down activities because those two similar activities are often confused with one another. Our results indicate that none of the eight learning algorithms consistently performs best, but the logistic regression classifier does perform best overall.

The most important activities to analyze are the climbing up and climbing down activities. The confusion matrices indicate that many of the prediction errors are due to confusion between these two activities. If we focus on the results for the DT model, when they are climbing up and climbing down, the most common incorrect classification occurs when we predict climbing down and climbing up, which accounts for a decrease in accuracies of 19.5% and 22.9%, respectively. On the other hand, using air pressure data, the activities of standing up, sitting down, climbing up, and climbing down have been recognized with more than 99% of accuracy as shown in Table IV. Such high accuracy is required for building safety applications based on for instance, falling, and climbing up detection.

IV. CONCLUSION

This paper has presented the activity recognition method for children using only a triaxial accelerometer and a barometric pressure sensor. Time-domain and frequency-domain features are extracted for categorizing body postures such as standing still and wiggling as well as locomotion such as toddling and crawling. To improve the performance of the child activity recognition method, six features including magnitude, mean, standard deviation, slope, energy, and correlation are extracted from the preprocessed signals. Multiple feature sets are compared to find an optimized classification method, and showed how well they performed on a body.

The average overall accuracies of the SVM and DT are 86.2% and 88.3%, respectively, with acceptable computational complexity using only a wearable triaxial accelerometer sensor. In addition, the average overall accuracies of the SVM and DT are 98.43% and 96.3%, respectively, with acceptable computational complexity using a wearable triaxial accelerometer and a barometric pressure sensor. Our proposed method including the pressure information demonstrated an improved performance in detecting climbing up and down activities. Results showed that using a barometric pressure sensor could reduce the incidence of false alarms. The early warning system will give the parents enough time to save their babies, and, thus, minimize any instances of falling accidents or sudden infant death syndrome.

ACKNOWLEDGMENT

The authors would like to thank all the volunteers who participated in our experiments. They would also like to thank D. Greco for previewing our manuscript.

REFERENCES

[1] A. M. Khan, Y.-K. Lee, S. Y. Lee, and T.-S. Kim. (2010, Sep.). A triaxial accelerometer-based physical-activity recognition via augmented-signal features and a hierarchical recognizer. *Trans. Info. Tech. Biomed.*, [Online]. *14(5)*, pp. 1166–1172, Available: http://dx.doi.org/10.1109/TITB.2010.2051955

[2] N. Li, Y. Hou, and Z. Huang. (2011). A real-time algorithm based on triaxial accelerometer for the detection of human activity state. in *Proc. 6th Int. Conf. Body Area Netw.*, ser. BodyNets '11. ICST, Brussels, Belgium, Belgium: ICST (Institute for Computer Sciences, Social-Informatics and Telecommunications Engineering), [Online]. pp. 103–106, Available: http://dl.acm.org/citation.cfm?id=2318776.2318801

[3] A. G. Bonomi. (2011). Physical activity recognition using a wearable accelerometer. in *Proc. Sens. Emot.*, ser. Philips Research Book Series, J. Westerink, M. Krans, and M. Ouwerkerk, Eds., Springer Netherlands, [Online]. vol. 12, pp. 41–51. Available: http://dx.doi.org/10.1007/978-90-481-3258-4_3

[4] S. Boughorbel, J. Breebaart, F. Bruekers, I. Flinsenberg, and W. ten Kate. (2010). Child-activity recognition from multi-sensor data. in *Proc. 7th Int. Conf. Methods Tech. Behav. Res.*, ser. MB '10. New York, NY, USA: ACM, [Online]. pp. 38:1–38:3, Available: http://doi.acm.org/10.1145/1931344.1931382

[5] A. Fleury, M. Vacher, and N. Noury, "Svm-based multimodal classification of activities of daily living in health smart homes: Sensors, algorithms, and first experimental results," *IEEE Trans. Inf. Technol. Biomed.*, vol. 14, no. 2, pp. 274–283, Mar. 2010.

[6] C. Zhu and W. Sheng. (2009). Multi-sensor fusion for human daily activity recognition in robot-assisted living. in *Proc. 4th ACM/IEEE Int. Conf. Human Robot Int.*, ser. HRI '09. New York, NY, USA: ACM, [Online]. pp. 303–304, Available: http://doi.acm.org/10.1145/1514095.1514187

[7] L. Atallah, B. Lo, R. King, and G.-Z. Yang, "Sensor positioning for activity recognition using wearable accelerometers," *IEEE Trans. Biomed. Circuits Syst.*, vol. 5, no. 4, pp. 320–329, Aug. 2011.

[8] L. Bao and S. S. Intille. (2004). Activity recognition from user-annotated acceleration data. *Pervas. Comput.*, [Online]. pp. 1–17, Available: http://www.springerlink.com/content/9aqflyk4f47khyjd

[9] R. Luo and M. Kay, "Multisensor integration and fusion in intelligent systems," *IEEE Trans. Syst., Man, Cybern.*, vol. 19, no. 5, pp. 901–931, Sep./Oct. 1989.

[10] R. R. Brooks and S. S. Iyengar, *Multi-sensor Fusion: Fundamentals and Applications With Software*. Englewood Cliffs, NJ: Prentice-Hall, 1998.

[11] R. Luo, C.-C. Yih, and K. L. Su, "Multisensor fusion and integration: Approaches, applications, and future research directions," *IEEE Sensors J.*, vol. 2, no. 2, pp. 107–119, Apr. 2002.

[12] N. Ravi, N. Dandekar, P. Mysore, and M. L. Littman. (2005). Activity recognition from accelerometer data. in *Proc. 17th Conf. Innovat. Appl. Artif. Intell.*, AAAI Press, [Online]. vol. 3, pp. 1541–1546, Available: http://dl.acm.org/citation.cfm?id=1620092.1620107

[13] B. Baas and S. U. D. of Electrical Engineering. (1999). *An Approach to Low-Power, High-Performance, Fast Fourier Transform Processor Design*. Stanford, CA: Stanford University. [Online]. Available: http://books.google.com/books?id=61KFHwAACAAJ

[14] R. Kohavi. (1995). A study of cross-validation and bootstrap for accuracy estimation and model selection. in *Proc. 14th Int. Joint Conf. Artif. Intell.*, Francisco, CA, USA: Morgan Kaufmann Publishers Inc., [Online]. vol. 2, pp. 1137–1143, Available: http://dl.acm.org/citation.cfm?id=1643031.1643047

[15] J. R. Quinlan, *C4.5: Programs for Machine Learning (Morgan Kaufmann Series in Machine Learning)*, 1st ed. San Mateo, CA: Morgan Kaufmann, Oct. 1992.

[16] J. C. Platt. (1999). Fast training of support vector machines using sequential minimal optimization, *Advances in kernel methods.*, B. Schölkopf, C. J. C. Burges, and A. J. Smola, Eds., Cambridge, MA: MIT Press. [Online]. pp. 185–208, Available: http://dl.acm.org/citation.cfm?id=299094.299105

[17] S. S. Keerthi, S. K. Shevade, C. Bhattacharyya, and K. R. K. Murthy. (2001, Mar.). Improvements to platt's SMO algorithm for SVM classifier design. *Neur. Comput.*, [Online]. *13(3)*, pp. 637–649, Available: http://dx.doi.org/10.1162/089976601300014493

[18] F. Foerster, M. Smeja, and J. Fahrenberg. (1999, Sep.). Detection of posture and motion by accelerometry: A validation study in ambulatory monitoring. *Comput. Human Behav.*, [Online]. *15(5)*, pp. 571–583, Available: http://dx.doi.org/10.1016/S0747-5632(99)00037-0

[19] G. H. John and P. Langley. (1995). Estimating continuous distributions in bayesian classifiers. [Online]. pp. 338–345, Available: http://citeseerx.ist.psu.edu/viewdoc/summary?doi=10.1.1.8.3257

[20] K. Aminian, P. Robert, E. Buchser, B. Rutschmann, D. Hayoz, and M. Depairon. (1999, May). Physical activity monitoring based on accelerometry: validation and comparison with video observation. *Med. Biol. Eng. Comput.*, [Online]. *37(3)*, pp. 304–308, Available: http://dx.doi.org/10.1007/BF02513304

[21] I. H. Witten and E. Frank, *Data Mining: Practical Machine Learning Tools and Techniques* (Morgan Kaufmann Series in Data Management Systems). 2nd ed. San Francisco, CA, : Morgan Kaufmann, 2005.

[22] M. A. McDowell, C. D. Fryar, C. L. Ogden, and K. M. Flegal. (2008). Anthropometric reference data for children and adults: United States, 2003—2006. U.S. Department of Health and Human Services, Centers for Disease Control and Prevention, [Online]. Available: http://www.cdc.gov/nchs/data/nhsr/nhsr010.pdf.

Yunyoung Nam received the B.S., M.S., and Ph.D. degrees in computer engineering from Ajou University, Suwon, Korea in 2001, 2003, and 2007, respectively.

He was a Senior Researcher in the Center of Excellence in Ubiquitous System from 2007 to 2009. He was a Research Professor in Ajou University . He also spent time as a Visiting Scholar at Center of Excellence for Wireless & Information Technology (CEWIT), Stony Brook University, New York. He is currently a Postdoctoral Researcher at Stony Brook University. His research interests include multimedia database, ubiquitous computing, image processing, pattern recognition, context-awareness, conflict resolution, wearable computing, intelligent video surveillance, and cloud computing.

Jung Wook Park received the B.S. and M.S. degrees in electronics engineering from Ajou University, Suwon, Korea, in 2007 and 2010, respectively.

He is currently a Research Engineer at LG Electronics, Seoul, Korea. He was a Visiting Researcher at Mobile and Pervasive Computing Laboratory, the University of Florida. His research interests include pervasive computing, human activity recognition, and assistive technology.